DOI: 10.7860/JCDR/2025/81070.21937



Histological and Histochemical Analysis of Foetal Suprarenal Gland Maturation from 13-40 Weeks of Gestation: An Observational Study

JIBY LIVINGTA HERBERT¹, RADHIKA J KRISHNAN², CD ANAND³, SUNDARAPANDIAN SUBRAMANIAN⁴, BALAKRISHNAN RAMAMOORTHY⁵, MOHAMMED JUNAID HUSSAIN DOWLATH⁶



ABSTRACT

Introduction: The Suprarenal Glands (SRG), a pair of endocrine glands located at the upper poles of the kidneys, originate from different developmental origins. The glands are divided into an outer cortex and an inner medulla. The cortex is further divided into the Zona Glomerulosa (ZG), Zona Fasciculata (ZF) and Zona Reticularis (ZR) while the medulla contains chromaffin cells—specialised neuroendocrine cells that synthesise and secrete catecholamines such as epinephrine and norepinephrine. These cells are also being studied for their regenerative applications in treating neurodegenerative diseases, including Parkinson's disease.

Aim: To identify the histological features of the foetal suprarenal cortex and medulla, track changes during development and measure the number of chromaffin cells at various developmental stages.

Materials and Methods: This observational study was conducted from February 2024 to January 2025 in the Department of Anatomy, SRM Medical College Hospital and Research Centre, Chennai, Tamil Nadu, India. Thirty-two foetuses of gestational ages 13–40 weeks were collected. The gestational age of the foetuses was estimated by Crown–Rump Length (CRL) and they were grouped into four groups (I–IV). The tissues from each

sample were collected, processed and sectioned for histology and histochemical procedures. Images of the sections were captured with an inverted microscope attached to a CCD camera and these images were analysed using ImageJ software. The parameters measured included the thickness of the ZG, ZF, ZR and the medulla and the number of chromaffin cells. Statistical analysis was performed using Statistical Package for the Social Sciences (SPSS) version 25.0.

Results: The cortex becomes progressively thinner with increasing gestational age. The medulla, on the other hand, shows an increase in thickness beginning around the late second trimester and reaches its maximum by the late third trimester. The right SRG showed a gradual increase in chromaffin cells up to the late second trimester, with around a 30–35% decrease in the early third trimester. The left gland showed a gradual increase in chromaffin cells from the early second trimester, reaching around a 50% increase by the late third trimester.

Conclusion: The findings suggest functional and developmental asymmetries between the foetal SRGs, with the left gland undergoing more significant changes compared to the right. This asymmetry may have implications for understanding foetal stress responses and the maturation of neuroendocrine regulation.

Keywords: Adrenal glands, Anatomy and histology, Chromaffin cells, Foetal development, Foetus, Gestational age

INTRODUCTION

The SRG, or adrenal glands, are a pair of endocrine organs located at the superior poles of the kidneys, enclosed by the renal fascia [1] but separated from the kidneys by a thin layer of loose connective tissue [2]. These glands play a crucial role in homeostasis by regulating metabolism, the immune response and the stress response through hormone secretion. Structurally, each gland comprises two functionally and embryologically distinct regions: the outer cortex, derived from the mesoderm and the inner medulla, which originates from neural crest cells [1].

At birth, the SRGs are relatively large, measuring approximately one third the size of the corresponding kidney due to the prominent development of the foetal zone in the cortex [1]. The foetal zone is responsible for producing dehydroepiandrosterone (DHEA), a precursor of placental oestrogen, which is essential for maintaining pregnancy [3]. Following birth, the foetal zone rapidly shrinks, leading to a marked reduction in gland size; more than half its birth weight is lost within the first two months. The adrenal cortex gradually reorganises, resuming growth by the second year of life and attaining adult dimensions by puberty, with minimal further increase in weight throughout adulthood [2].

Embryologically, the adrenal gland develops from two distinct origins [4]. The cortex is derived from coelomic mesothelium around 5-6 weeks of gestation, initially forming a primitive foetal cortex [5]. By the ninth week, the cortex differentiates into two zones: the outer definitive zone and the inner foetal zone. During the third trimester, a transitional zone emerges, further contributing to the structural reorganisation of the postnatal gland [6]. Eventually, the definitive cortex gives rise to three histologically distinct zones: ZG, ZF and ZR [7].

In contrast, the adrenal medulla originates from sympathochromaffin cells, derived from neural crest cells. These chromaffin cells, rich in catecholamine granules, are arranged in clusters or cords and stain dark brown with chromaffin salts, indicating the presence of epinephrine and norepinephrine. Functionally, the medulla serves as an extension of the sympathetic nervous system, crucial for the "fight-or-flight" response [8].

Kastriti et al., have provided new insights into adrenal medulla development, revealing that chromaffin cell precursors arise from Schwann cell precursors, which detach from neural structures and diversify into chromaffin subpopulations, thereby enhancing our understanding of medullary ontogeny [9]. Moreover, SOX2+ sustentacular cells have been identified as a postnatal

stem cell population capable of differentiating into chromaffin cells and maintaining medullary homeostasis via paracrine WNT6 signalling [10].

Although prior studies have characterised adrenal development [11,12], high-resolution histological and histochemical mapping of foetal adrenal maturation from early to late gestation remains limited. Moreover, the plasticity of chromaffin cells—particularly their potential in neuroendocrine regeneration and relevance to treating neurodegenerative conditions—has yet to be fully elucidated. Thus, this study presents a detailed timeline of the structural and cellular maturation of the foetal SRG from 13 to 40 weeks of gestation, focusing on morphometric changes in cortical zones and chromaffin cell distribution.

MATERIALS AND METHODS

This observational study was conducted in the Department of Anatomy in collaboration with the Department of Obstetrics and Gynaecology, SRM Medical College Hospital and Research Centre, Chennai, Tamil Nadu, India, from February 2024 to January 2025. The study involved histological and histochemical examination of foetal SRGs. Ethical clearance was obtained from the Institutional Ethics Committee (IEC approval no: SRMIEC-ST1123-1352).

Inclusion criteria: A total of 32 foetuses aborted, stillborn, or with Intrauterine Death (IUD), ranging from 13 to 40 weeks of gestation, were collected. All foetuses were embalmed immediately after collection using standard embalming procedures to ensure tissue preservation.

Exclusion criteria: Foetuses resulting from spontaneous abortions or IUDs without any gross congenital malformations, urogenital anomalies, or maternal history of endocrine disorders to avoid potential confounding variables affecting adrenal development were excluded from the study.

Sample size: The sample size was determined by complete enumeration, as all eligible foetal specimens available during the study period were included, resulting in a final sample size of 32 foetuses.

Study Procedure

Gestational age was determined using CRL measurements, following established foetal biometry standards [13]. CRL was chosen as it is the most accurate and standardised parameter for estimating gestational age in early to mid-gestation, particularly before the influence of foetal growth variability sets in [14]. The foetuses were categorised into four groups based on gestational age to facilitate comparative analysis of glandular maturation. Classification was Group 1: Early second trimester (13-19 weeks), Group 2: Late second trimester (20-27 weeks), Group 3: Early third trimester (28-33 weeks) and Group 4: Late third trimester (34-40 weeks). The grouping of foetuses into trimester-based categories aligns with established developmental milestones, aiding in the systematic evaluation of glandular maturation [15].

The foetuses were aligned according to gestational age for easy identification, as shown in [Table/Fig-1]. A Y-shaped incision was



[Table/Fig-1]: Foetuses arranged based on their gestational age

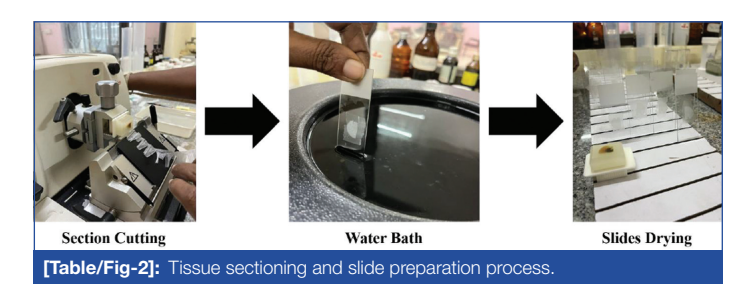
made in the anterior abdominal wall, following standard cadaveric dissection protocols. The peritoneum and fascia covering the kidneys and SRGs were carefully dissected to expose the glands, ensuring preservation of adjacent structures. The SRGs were excised bilaterally, with minimal disruption to the surrounding tissues. The collected glandular tissues were then placed in a sterile container filled with 10% neutral buffered formalin for fixation and preservation for 24-48 hours, following standard anatomical dissection and histological processing techniques [16].

The fixed tissue samples were then wrapped in filter paper bearing the identification label. Further processing of the tissues proceeded as follows: an automated tissue processor was used for chemical processing and paraffin embedding. Tissues were placed in cassettes and dehydrated using 100% acetone for one hour with three changes at 20-minute intervals. Acetone was chosen over ethanol for dehydration due to its faster action and efficiency in lipidrich tissues like the adrenal gland, minimising tissue shrinkage and better preserving morphology. This was followed by xylene for one hour, with two changes of 30 minutes each.

This section describes the tissue processing and analysis workflow. The dehydrated tissues were transferred to molten paraffin at 54–56°C and allowed to infiltrate for two hours. The infiltrated tissues were placed in an L-shaped embedding mold containing melted paraffin and left to cool and solidify. After solidification, the hardened paraffin blocks were retrieved and prepared for sectioning.

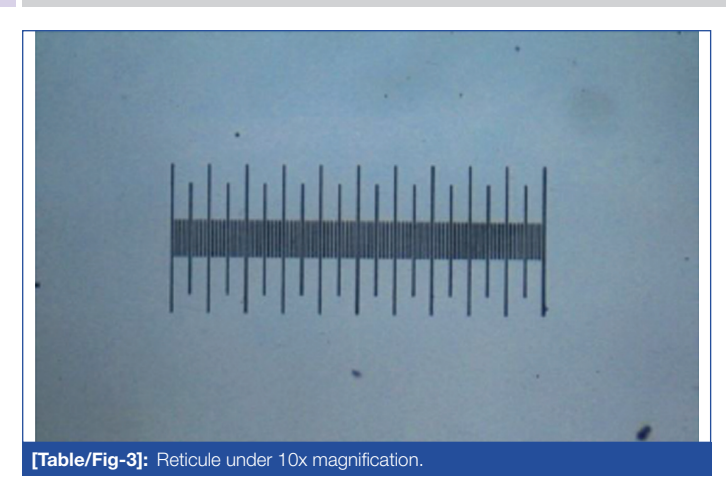
The paraffin blocks were trimmed and then mounted on a microtome. Sections were cut at a thickness of 5 μm and ribbons were floated on a water bath before being mounted on poly-L-lysine-coated, aluminized slides. Five-micron sections were selected to balance structural clarity and ease of handling during histochemistry. Sections thinner than 5 μm could enhance resolution but increase the risk of tearing and incomplete antigen retrieval in dense foetal tissues.

Slides were then dried and labeled appropriately for examination [Table/Fig-2]. Haematoxylin and Eosin (H&E) staining was applied to the histological sections to improve visualisation of cellular structures. The staining process included deparaffinisation through a series of xylene treatments, followed by rehydration with graded alcohol solutions. The sections were immersed in Harris Hematoxylin for 4-5 minutes, rinsed with tap water and then subjected to acidalcohol differentiation for 5-30 seconds. A bluing step using 1% lithium carbonate was performed, followed by counterstaining the sections with Eosin Y for two minutes. The stained sections underwent rapid dehydration with absolute alcohol, were cleared in xylene and were subsequently mounted using DPX mounting medium with coverslips.



For histochemical analysis, Chromogranin A immunostaining was used to identify neuroendocrine components and assess cellular differentiation. Chromogranin A is a well-established neuroendocrine marker expressed in secretory granules of chromaffin cells, thus serving as a reliable indicator of medullary differentiation.

Microscopic examination of histological and histochemical sections was performed using a confocal microscope at $4\times$ and $10\times$ magnifications. The captured images were imported into ImageJ, converted to 8-bit and the threshold adjusted for each image. Scale bars were calibrated using a reticule [Table/Fig-3]. Cells were analysed using the "Convert to Mask," "Make Binary," and



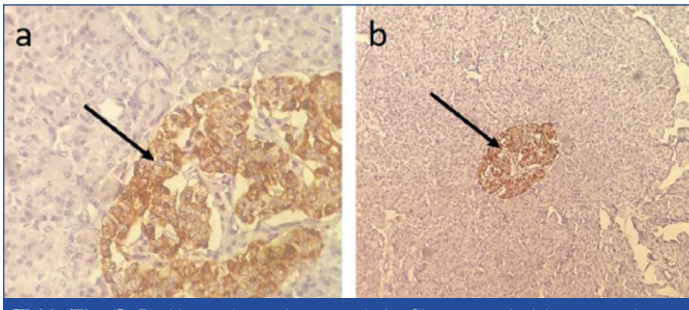
"Watershed" functions. The number of cells was quantified using the "Analyse Particles" option. The arrow (line) tool was used to measure the thickness of the layers separately.

STATISTICAL ANALYSIS

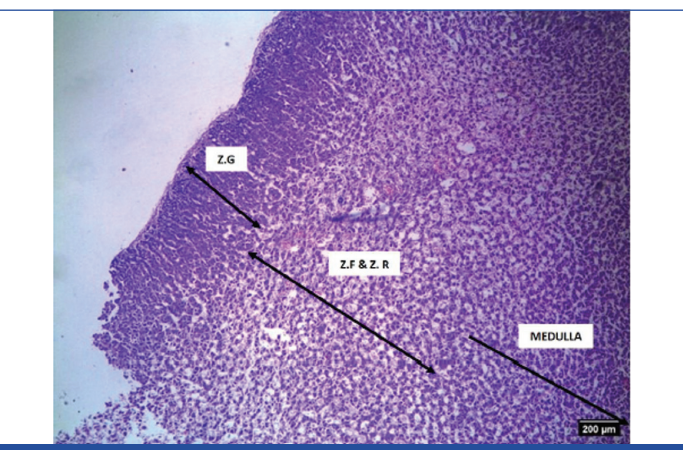
All statistical analyses were performed using SPSS version 25.0.

RESULTS

Identification: The capsule was identified by the presence of connective tissue, fibers and blood vessels. Chromogranin A immunoreactivity was validated using pancreatic tissue as a control. The islets of Langerhans demonstrated strong positive immunostaining, confirming antibody specificity, while the surrounding exocrine pancreatic tissue showed no immunoreactivity, serving as an internal negative control [Table/Fig-4]. Histological images were observed for Groups 1-4 and are presented in [Table/Fig-5-8].

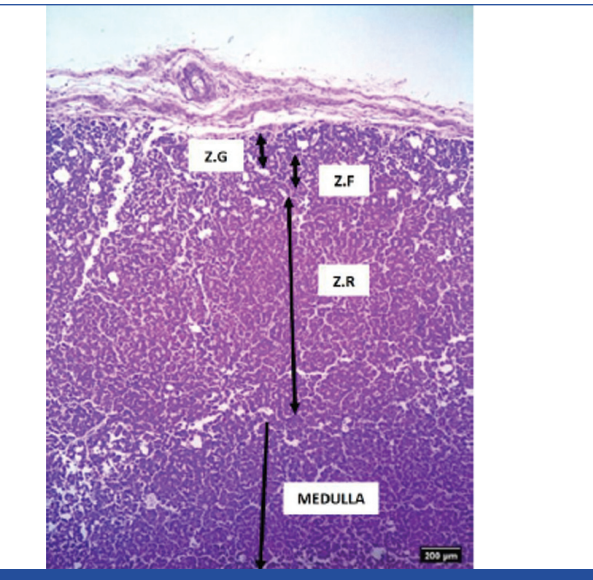


[Table/Fig-4]: Positive and negative controls for Chromogranin A immunostaining (a-40x magnification, b-10x magnification). Pancreatic tissue showing strong Chromogranin A positivity in the islets of Langerhans (arrow), confirming staining specificity. The adjacent exocrine pancreas shows no immunoreactivity, validating the negative control.

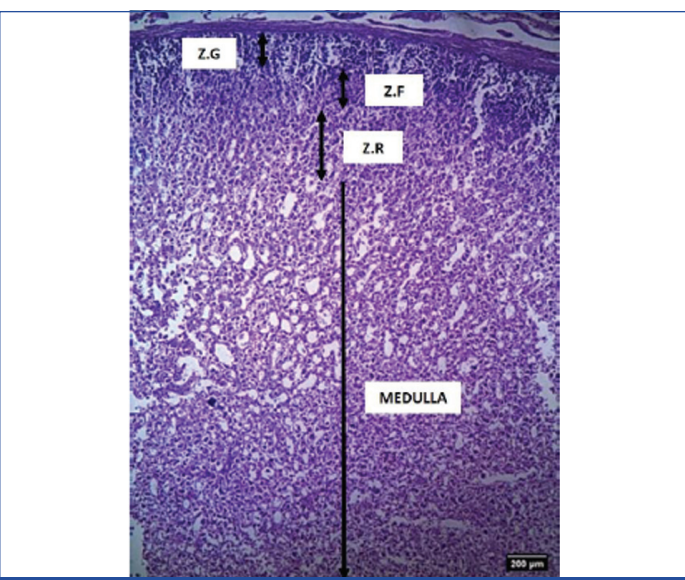


[Table/Fig-5]: Histological image of SRG with arrows representing ZG, ZF, ZR and Medulla of Group 1 in 4x magnification.

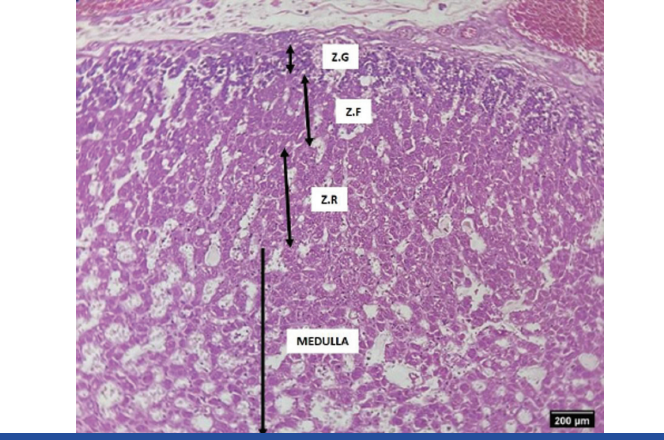
ZG: The outermost layer, located near the capsule. The cells are arranged in small, inverted U-shaped or acinar-like groups. They are polyhedral or columnar in shape, with cytoplasm that stains blue (basophilic) and with visible nuclei.



[Table/Fig-6]: Histological image of SRG with arrows representing ZG, ZF, ZR and Medulla of Group 2 in 4x magnification.



[Table/Fig-7]: Histological image of SRG with arrows representing ZG, ZF, ZR and Medulla of Group 3 in 4x magnification.



[Table/Fig-8]: Histological image of SRG with arrows representing ZG, ZF, ZR and Medulla of Group 4 in 4x magnification.

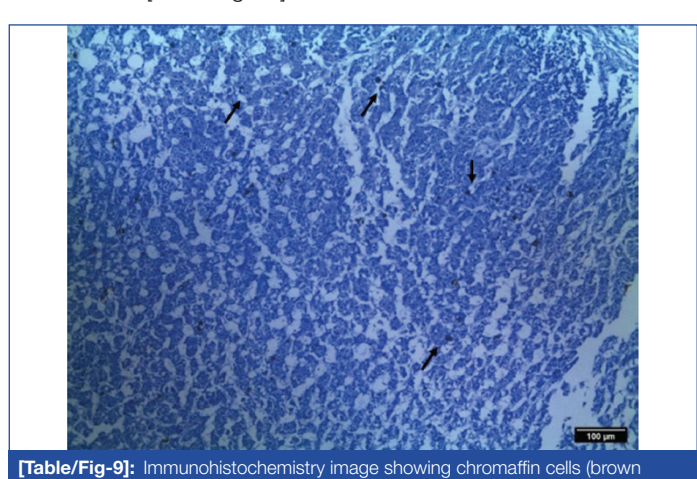
ZF: The cells are arranged in straight columns, two cells thick, with sinusoids interspersed between them. This layer constitutes the middle part of the cortex. The cells are polyhedral, featuring basophilic cytoplasm and vesicular nuclei. Due to the high lipid content in this layer, the lipids are removed during tissue processing, resulting in an empty, vacuolated appearance.

ZR: This is the innermost layer of the cortex. The cells are smaller and more acidophilic compared to the other two layers. Although it

resembles the zona fasciculata, it contains less lipid. The cytoplasm is eosinophilic.

Medulla: It consists of groups or columns of cells separated by wide sinusoids. The cells are either columnar or polyhedral in shape, with basophilic cytoplasm.

Histochemistry measurement of chromaffin cells, cortex, medulla and capsular thickness. Immunohistochemistry image showing chromaffin cells is shown in [Table/Fig-9]. The values of the cortex, medulla and capsular thickness were measured using ImageJ software and are shown in [Table/Fig-10]. The cells were visualised under 4× and 10× magnification. Thickness of ZG, ZF and ZR: The thickness of all three layers was calculated using ImageJ software. The images were viewed under 4× and 10× magnification. In Group I, the ZF and ZR were indistinguishable, so their values were combined. The thickness of ZG, ZF and ZR for Groups II, III and IV are shown in [Table/Fig-11].



Chromaffin cell distribution using histochemistry: The number of chromaffin cells per square field in each trimester was determined using histochemistry (HC). The results are summarised in [Table/Fig-12].

pigmented cells)

DISCUSSION

The development of the foetal SRG is a dynamic process influenced by gestational age [17]. A study by Kumar TS et al., has shown that the cortex becomes distinctly defined by 18 weeks and thickens progressively until term. This thickening is accompanied by the formation of blood vessels in the capsule as early as 15 weeks, suggesting a role in the gland's vascularisation and functionality. The foetal cortex shows progressive thickening with advancing gestational age, accompanied by persistent lymphocytic infiltrates in the permanent cortex. This further supports the notion of an evolving immune interaction within the gland [18].

Interestingly, this study contrasts with Chan WH et al., which demonstrated progressive thinning of the cortex with increasing gestational age [19]. This suggests that while the early gestational period is marked by cortical expansion, later stages may involve remodelling or regression of specific cortical layers. The medulla, on the other hand, shows a significant increase in thickness, beginning around the late second trimester and reaching its maximum by the late third trimester. This aligns with the gland's increasing functional demand in preparation for postnatal life [19].

Among the cortical zones, the ZG maintains a steady increase in thickness from the early second trimester. However, ZF and ZR exhibit exponential increases from the late second trimester, emphasising that these zones undergo rapid expansion to support the synthesis of essential steroid hormones. Notably, the ZR contributes the majority to cortical thickness in the later stages, possibly preparing the gland for the shift from foetal to postnatal endocrine function.

The HC analysis of this study shows two distinct peaks in chromaffin cell distribution, one occurring in the late second trimester and another extending into birth in the late third trimester. This biphasic pattern suggests an active phase of differentiation and proliferation of chromaffin cells, which could be linked to the increasing demand for catecholamines as the foetus approaches term [20].

Zona Glomerulosa, Zona Fasciculata, Zona Reticularis: Korukonda S and Prusti JS, found that the capsule became distinctly

Parameters	Range (µm) (Mean±SD)				
	Group 1	Group 2	Group 3	Group 4	
Cortex thickness: Right	324.51-739.3	509.78-1469.81	570.37-945.79	244.44-2353.44	
	(444.07±149.68)	(874.64±338.62)	(732.85±147.63)	(1299.39±645.65)	
Cortex thickness: Left	293.14-594.24	408.43-1333.02	304.39-1417.72	647.42-2229.71	
	(490.83±136.27)	(840.75±326.49)	(608.3±396.47)	(1468±571.28)	
Medulla thickness: Right	1326.40-6766.1	841.41-8657.07	1489.79-9121.12	965.78-5226.7	
	(4538.66±2198.51)	(3611.69±2963.94)	(5801.54±2728.41)	(2240.66±1611.31)	
Medulla thickness: Left	1624.30-5089.29	2292.76-7161.51	666.14-3104.29	234.93-8530.56	
	(3172.91±1502.16)	(4723.51±1929.04)	(2270.12±940.62)	(2992.03±2977.72)	
Capsule thickness: Right	78.08-566.38	60.94-256.54	81.62-133.46	98.09-301.45	
	(392.15±180.34)	(153.72±80.58)	(112.09±19.67)	(3157.57±9482.52)	
Capsule thickness: Left	509.78-1469.81	76.20-249.65	55.75-201.03	102.50-396.69	
	(147.72±102.76)	(119.3±56.14)	(150.35±61.24)	(182.91±95.49)	

[Table/Fig-10]: Cortical thickness increases with gestation, peaking in the late third trimester-more prominently on the left. Medullary thickness fluctuates, highest in early third trimester on the right. Capsular thickness shows no consistent pattern across groups.

	Range (μm) (Mean±SD)					
Parameters	Group 1	Group 2	Group 3	Group 4		
ZG: Right	109.7-276.47 (173.66±51.71)	66.73-162.41 (114.85±30.97)	109.57-185.21 (134.55±26.39)	51.54-180.59 (108.15±34.9)		
ZG: Left	101.45-259.31 (151.42±68.76)	67.23-199.10 (135.98±58.02)	60.52-135.71 (103.87±31.12)	67.83-190.99 (118.69±32.66)		
ZF: Right	160.81-462.83 (262.49±102.81)	89.74-520.28 (628.12±333.72)	88.07-235.57 (461.55±105.8)	78.46-499.45 (912.87±586.14)		
ZR: Right		208.70-1108.10 (252.62±175.77)	326.20-622.88 (136.61±57.98)	114.44-1904.46 (284.57±119.92)		
ZF: Left	77.36-491.95 (276.65±162.23)	120.56-523.01 (716.22±227.2)	76.58-214.76 (374.95±377.74)	118.27-524.98 (980.75±485.37)		
ZR: Left		406.40-902.24 (293.42±168.92)	117.86-1167.34 (129.99±44.15)	154.94-1650.50 (368.55±166.37)		

[Table/Fig-11]: ZG thickness declines slightly across trimesters. ZF and ZR exhibit progressive thickening with gestational age, with the most significant (p<0.05) increase in ZR during the late 3rd trimester, especially on the left-side.

	Range (cells per square field) (Mean±SD)				
Parameters	Group 1	Group 2	Group 3	Group 4	
HC: Right	5423-9198	7071-15326	4785-9742	6331-15233	
	(7271.14±1397.13)	(9700.5±3311.03)	(7242.71±2016.94)	(9887.7±2650.68)	
HC: Left	4523-12135	5432-18419	7054-8963	7168-14954	
	(7466±2725.117)	(9928±5272.45)	(8039.86±755.86)	(11433.7±2379.49)	

[Table/Fig-12]: Chromaffin cell count per square field shows an increase with gestational age, with higher counts observed in the left adrenal gland during the late 3rd trimester.

identifiable by 12 weeks, with progressive thickening throughout gestation. By 24 weeks, trabeculae containing blood vessels extend from the capsule into the cortex, further supporting the hypothesis that vascularisation is a critical factor in SRG development [21]. In this study, the capsule thickness also showed a progressive increase, reaching its peak by the late third trimester. This was in line with Rao RM et al., suggesting that capsule development plays a pivotal role in supporting the expansion of underlying cortical zones [22]. Rao M et al., described the SRG as initially larger than the kidney at 16 weeks, followed by a reduction in size at birth due to involution and necrosis, resulting in about a 50% reduction within 2-3 weeks. This study observed a larger left SRG compared to the right and a gradual increase in gland size, consistent with prior findings [22].

Microscopic analysis identified two cortical regions with distinct parenchymal cells and confirmed differentiation of chromaffin cells by 12 weeks and ganglionic cells by 28 weeks. Developmental changes in cortical zones were also noted [23]. This corroborates the findings of this study, particularly in demonstrating that the left SRG tends to be larger than the right, an asymmetry also noted in previous studies. This size difference could be attributed to variations in vascular supply and differential hormonal demands between the two sides.

The ZG develops first, during adrenal differentiation and shows consistent growth but at a slower pace. ZG growth stabilises early postnatally, maintaining its primary role in mineralocorticoid production. The ZF shows an asymmetric development pattern and expands significantly after birth to meet the increasing cortisol demand necessary for metabolic adaptation. The ZR does not show statistically significant differences between the left and right glands, suggesting a relatively uniform development pattern across both sides. It is important to acknowledge that variations in foetal SRG morphology may be influenced by confounding factors such as the cause of foetal death, postmortem interval and intrauterine growth restriction. For instance, congenital adrenal hyperplasia (CAH) leads to cortical hyperplasia, loss of zonation and lipid deposits due to defective steroid synthesis [24]. Similarly, pheochromocytoma, though rare in foetuses, arises from chromaffin cells and can compress the cortex, causing thinning [25]. While obvious anomalies were excluded, subtle or undetected conditions may have influenced gland morphology in some cases.

Suprarenal medulla-Chromaffin cells using histochemistry: The adrenal medulla originates from neural crest-derived chromaffin cells, which undergo differentiation and proliferation during gestation [26]. A study by Bocian-Sobkowska J et al., showed that the adrenal medulla volume increased gradually until the 20th week, then expanded rapidly until the 31st week of foetal development [27]. They also observed a consistent, linear increase in the number of chromaffin cells throughout the study period. In contrast, the average size of the adrenal medullary cells remained constant until the 17th week, after which it gradually increased linearly until the 31st week, after which it plateaued by the end of intrauterine development [27]. This trend supports the hypothesis that the adrenal medulla reaches near-functional maturity by the late third trimester. This study further refines this timeline by demonstrating distinct laterality in chromaffin cell development. The right suprarenal gland showed a gradual increase in chromaffin cells up to the late 2nd trimester, followed by a 30-35% decrease in the early 3rd trimester. This suggests a possible phase of cellular remodeling or apoptosis, which may be necessary for medullary reorganisation before birth. Conversely, the left gland exhibits a gradual increase in chromaffin cells from early 2nd trimester, with around a 50% increase by the late 3rd trimester. This discrepancy between the right and left sides may be due to several factors: differences in innervation patterns between the two glands leading to asymmetric neural stimulation, variations in vascularisation which could influence nutrient and oxygen supply to chromaffin progenitor cells and functional specialisation, where one side may be more involved in immediate catecholamine synthesis while the other undergoes structural reorganisation.

The results of this study offer new insights into the development of the foetal SRG, specifically concerning the varying growth patterns of cortical zones and chromaffin cells. Previous literature has largely concentrated on gross anatomical changes [18]; however, histological and histochemical analyses in this study provide a more detailed understanding of the cellular and molecular dynamics within the gland. Furthermore, this study has documented the distribution of chromaffin cells in the adrenal glands, which can support further clinical studies in this field.

The asymmetry in chromaffin cell distribution may be influenced by HIF-1 α , which regulates catecholamine production and responds to intrauterine oxygen levels. Uneven HIF-1 α activity between the two glands-possibly due to differences in blood supply which might cause side-specific development [28]. Also, neural crest cell migration, controlled by pathways like Notch, could show left-right bias, leading to unequal chromaffin cell formation [29]. Future studies on these pathways may help explain adrenal asymmetry.

Further research, especially focusing on molecular markers and transcriptomic profiling, may clarify the genetic and epigenetic mechanisms that regulate SRG maturation. Longitudinal studies linking prenatal adrenal development to neonatal and postnatal endocrine function may yield important clinical insights, particularly regarding congenital adrenal disorders and foetal stress responses.

Limitation(s)

The limitations of this study include the indistinct appearance of the ZR and ZF in the early second trimester. Hence, a combined measurement was performed.

CONCLUSION(S)

The results of this study offer important insights into the developmental progression of the foetal SRG, specifically regarding the cortex, medulla and capsule. Cortical thickness shows a progressive decline with increasing gestational age, while medullary thickness begins to increase in the late second trimester and peaks by the late third trimester. The ZG demonstrates consistent growth beginning in the early second trimester among the cortical zones. The ZF and ZR exhibit an exponential increase in thickness from the late second trimester. The ZR forms the majority of cortical thickness when the ZF and ZR are considered together. The distribution of chromaffin cells in the right SRG shows a gradual increase until the late $2^{\rm nd}$ trimester, after which there is a decline to approximately 30-35% in the early $3^{\rm rd}$ trimester. Conversely, the left SRG demonstrates a gradual increase in chromaffin cells from the early $2^{\rm nd}$ trimester, reaching around 50% by the late $3^{\rm rd}$ trimester.

These findings deepen the understanding of the structural maturation timeline of the foetal SRG and may serve as a valuable reference for identifying deviations in adrenal development during routine prenatal

assessments. Clinically, this knowledge may aid in the early diagnosis and monitoring of CAH, adrenal hypoplasia and other endocrine disorders. Future research could leverage advanced molecular techniques such as single-cell RNA sequencing to explore cellular heterogeneity and lineage-specific differentiation patterns within the foetal adrenal gland.

Acknowledgement

The authors are grateful for the support provided by Dr. R. Balaji, Associate Professor, Department of Pathology and Dr. Aamina Hussain, Assistant Professor, Department of Community Medicine, SRM Medical College Hospital and Research Centre, Tamil Nadu, India.

REFERENCES

- [1] Van Slycke S, Van Den Heede K, Vandenwyngaerden EA. Adrenal glands: Anatomy, physiology, and pathophysiology. In: Shifrin AL, Raffaelli M, Randolph GW, Gimm O. (eds) Endocrine surgery comprehensive board exam guide. Springer, Cham. 2021. Available from: https://doi.org/10.1007/978-3-030-84737-1_17.
- [2] Standring S. Suprarenal gland. In: Standring S, editor. Gray's Anatomy: The Anatomical Basis of Clinical Practice. 42nd ed. London: Elsevier; 2021. p. 1239-1243.e2.
- [3] Bhaumik S, Lockett J, Cuffe J, Clifton VL. Glucocorticoids and their receptor isoforms: Roles in female reproduction, pregnancy, and foetal development. Biology. 2023;12(8):1104. Available from: https://doi.org/10.3390/biology12081104.
- [4] Markam Y, Loh HK, Gupta M, Gupta N, Mehta V. Suprarenal glands: A morphometric analysis in adult Indian population. Natl J Clin Anat. 2024;13(4):190-93. Available from: https://doi.org/10.4103/NJCA.NJCA_16_24.
- [5] Krishna A, Jain M. Adrenal gland: Embryology and anatomy. In: Mishra AK, Agarwal A, Parameswaran R, Singh KR, editors. Endocrine Surgery: A South Asian Perspective. 1st ed. Boca Raton: CRC Press; 2022. p. 321-323.
- [6] Kant Narayan R, Kumar A, Verma M. The development and anatomy of adrenal glands [Internet]. Adrenal glands-the current stage and new perspectives of diseases and treatment. IntechOpen; 2024. Available from: http://dx.doi. org/10.5772/intechopen.108799.
- [7] Gartner LP. Endocrine system. In: Gartner LP, editor. Textbook of Histology. 5th ed. Philadelphia: Elsevier; 2021. p. 305-32.e2.
- [8] Nicolaides NC, Willenberg HS, Bornstein SR, Chrousos GP. Adrenal cortex: Embryonic development, anatomy, histology and physiology. In: Feingold KR, Ahmed SF, Anawalt B, et al., editors. Endotext [Internet]. South Dartmouth (MA): MDText.com, Inc.; 2000 [updated 2023 Jun 12; cited 2025 Jul 2]. Available from: https://www.ncbi.nlm.nih.gov/books/NBK279023/.
- [9] Kastriti ME, Kameneva P, Kamenev D, Dyachuk V, Furlan A, Hampl M, et al. Schwann cell precursors generate the majority of chromaffin cells in zuckerkandl organ and some sympathetic neurons in paraganglia. Front Mol Neurosci. 2019;12:6. Available from: https://doi.org/10.3389/fnmol.2019.00006.
- [10] Santambrogio A, Kemkem Y, Willis TL, Berger I, Kastriti ME, Faure L, et al. SOX2+ sustentacular cells are stem cells of the postnatal adrenal medulla. Nat Commun. 2025;16:16. Available from: https://doi.org/10.1038/s41467-024-55289-5
- [11] Annamraju MR, Boddeti RK, Velichety SD, Battalapalli SR. Study on the gestational age-related histogenesis of human fetal suprarenal glands. Asian J Med Sci. 2020;11(5):61-68.

- [12] Annamaraju MR, Velichety SD, Boddeti RK, Battalapalli SR. Histological study of normal human suprarenal gland of different age groups. Asian J Med Sci. 2021;12(4):110-17.
- [13] Dursun A, Kastamoni Y, Kacaroglu D, Yuzbasioglu N, Ertekin T. Morphometric development of the tongue in fetal cadavers. Surg Radiol Anat. 2020;42(1):03-08. Available from: https://doi.org/10.1007/s00276-019-02301-z.
- [14] Hadlock FP, Shah YP, Kanon DJ, Lindsey JV. Fetal crown-rump length: Reevaluation of relation to menstrual age (5-18 weeks) with high-resolution real-time US. Radiology. 1992;182(2):501-05. Available from: https://doi.org/10.1148/radiology.182.2.1732970.
- [15] Persaud TVN, Torchia MG. Development of suprarenal glands. In: Moore KL, Persaud TVN, Torchia MG, editors. The Developing Human: Clinically Oriented Embryology. 12th ed. Philadelphia: Elsevier; 2023. p. 225-64.
- [16] Detton AJ. Dissection of suprarenal gland. In: Tank PW, Detton AJ, editors. Grant's Dissector. 16th ed. Philadelphia: Wolters Kluwer Health; 2016. p. 140-45.
- [17] Pignatti E, du Toit T, Flück CE. Development and function of the fetal adrenal. Rev Endocr Metab Disord. 2023;24(1):05-21. Available from: https://doi.org/10.1007/ s11154-022-09756-3.
- [18] Kumar TS, Kumar SS, Rekha BM. A histological study on the developing adrenal gland in human foetuses. Natl J Clin Anat. 2021;10(2):79-83. Available from: https://doi.org/10.4103/NJCA.NJCA_38_20.
- [19] Chan WH, Komada M, Fukushima T, Southard-Smith EM, Anderson CR, Wakefield MJ. RNA-seq of isolated chromaffin cells highlights the role of sex-linked and imprinted genes in adrenal medulla development. Sci Rep. 2019;9(1):3929. Available from: https://doi.org/10.1038/s41598-019-40501-0.
- [20] Rusch JA, Layden BT, Dugas LR. Signalling cognition: The gut microbiota and hypothalamic-pituitary-adrenal axis. Front Endocrinol (Lausanne). 2023;14:1130689. Available from: https://doi.org/10.3389/ fendo.2023.1130689.
- [21] Korukonda S, Prusti JS. Histological study of foetal suprarenal cortex. J Evid Based Med Healthc. 2018;5(45):3144-48. Available from: http://dx.doi. org/10.18410/jebmh/2018/640.
- [22] Rao RM, Kishore SR, Kumar CR. Study of morphogenesis of suprarenal gland in human foetuses of different gestational ages. J Evol Med Dent Sci. 2015;4(31):5342-49.
- [23] Sathiya S. Morphometry and histogenesis of human fetal suprarenal gland in different gestational age groups. J Res Med Dent Sci. 2021;9(8):138-40.
- [24] Sharma L, Momodu II, Singh G. Congenital adrenal hyperplasia. [Updated 2025 Jan 27]. In: StatPearls [Internet]. Treasure Island (FL): StatPearls Publishing; 2025 Jan-. Available from: https://www.ncbi.nlm.nih.gov/books/NBK448098/.
- [25] Lehman KA, Zynger DL. Pheochromocytoma. In: Pathology Outlines.com [Internet]. Choy B, Gonzalez RS, Tretiakova M, editors. [cited 2025 Jul 4]. Available from: https://www.pathologyoutlines.com/topic/adrenalpheochromocytoma.html.
- [26] Bechmann N, Berger I, Bornstein SR, Steenblock C. Adrenal medulla development and medullary-cortical interactions. Mol Cell Endocrinol. 2021;528:111258. Available from: https://doi.org/10.1016/j.mce.2021.111258.
- [27] Bocian-Sobkowska J, Wozniak W, Malendowicz LK, Ginda W. Stereology of human fetal adrenal medulla. Histol Histopathol. 1996;11(2):389-93.
- [28] Kolesova H, Hrabalova P, Bohuslavova R, Abaffy P, Fabriciova V, Sedmera D, et al. Reprogramming of the developing heart by Hif1a-deficient sympathetic system and maternal diabetes exposure. Front Endocrinol. 2024;15:1344074.
- [29] Shtukmaster S, Huber K. The role of the Notch signalling pathway in regulating the balance between neuronal and nonneuronal cells in sympathetic ganglia and the adrenal gland. Plos One. 2023;18(2):0281486.

PARTICULARS OF CONTRIBUTORS:

- 1. Postgraduate Student, Department of Anatomy, SRM Medical College Hospital and Research Centre, Faculty of Medicine and Health Sciences, SRM Institute of Science and Technology, Chennai, Tamil Nadu, India.
- 2. Professor, Department of Anatomy, Vels Medical College and Hospital, Manjakaranai Village, Thiruvallur, Tamil Nadu, India.
- 3. Professor, Department of Pathology, SRM Medical College Hospital and Research Centre, Faculty of Medicine and Health Sciences, SRM Institute of Science and Technology, Chennai, Tamil Nadu, India.
- 4. Professor and Head, Department of Anatomy, SRM Medical College Hospital and Research Centre, Faculty of Medicine and Health Sciences, SRM Institute of Science and Technology, Chennai, Tamil Nadu, India.
- 5. Professor, Department of Anatomy, SRM Medical College Hospital and Research Centre, Faculty of Medicine and Health Sciences, SRM Institute of Science and Technology, Chennai, Tamil Nadu, India.
- 6. Assistant Professor, Department of Anatomy, SRM Medical College Hospital and Research Centre, Faculty of Medicine and Health Sciences, SRM Institute of Science and Technology, Chennai, Tamil Nadu, India.

NAME, ADDRESS, E-MAIL ID OF THE CORRESPONDING AUTHOR:

Dr. Balakrishnan Ramamoorthy,

SRM Medical College Hospital and Research Centre, Faculty of Medicine and Health Sciences, SRM Institute of Science and Technology, SRM Nagar, Kattankulathur, Kanchipuram, Chennai-603203, Tamil Nadu, India.

E-mail: drbalkris83@gmail.com

Plagiarism X-checker: Jun 10, 2025Manual Googling: Jul 23, 2025

• iThenticate Software: Aug 05, 2025 (8%)

PLAGIARISM CHECKING METHODS: [Jain H et al.]

ETYMOLOGY: Author Origin

EMENDATIONS: 7

AUTHOR DECLARATION:

- Financial or Other Competing Interests: None
- Was Ethics Committee Approval obtained for this study? Yes
- Was informed consent obtained from the subjects involved in the study? Yes
- For any images presented appropriate consent has been obtained from the subjects. No

Date of Submission: Jun 02, 2025 Date of Peer Review: Jun 23, 2025 Date of Acceptance: Aug 07, 2025 Date of Publishing: Nov 01, 2025